

Fabrication of nanoscale features on ultra-thin glass-based dielectrics via self-masking and preferential etching to enhance capacitance*

Amoghavarsha Mahadevegowda[#], Colin Johnston, and Patrick S Grant

Abstract— Flexible capacitors based on ultra-thin glass (30 μm thick) were fabricated and the effect of nanoscale surface modification on the dielectric properties was studied. The ultra-thin glass samples were partially masked by the deposition and self-organisation of Ag-islands and then preferentially etched to produce a controlled topography. The etching duration was varied and its effect on Ag content and dielectric properties were studied by employing atomic force microscopy (AFM), scanning electron microscopy and energy-dispersive X-ray spectroscopy (SEM-EDS), and impedance spectroscopy. The AFM studies revealed the presence of nanoscale ‘peaks’, which were distributed across the surface of the glass, that following etching showed enhanced capacitance. Surface modification of glass using self-organised nano-scale metal island masks is shown to be an effective route to enhance the use of ultra-thin glass in capacitor applications.

I. INTRODUCTION

Ultra-thin glass has been investigated as a potential dielectric material for capacitor applications due to its exceptional properties [1], [2], [3], [4]: dielectric constant $k \sim 6$, operating temperature $\sim 180^\circ\text{C}$, dissipation factor $\tan \delta \sim 0.35\%$, breakdown strength $\sim 700 \text{ kV mm}^{-1}$, and flexibility that enables roll-to-roll processing. An energy density of up to $\sim 35 \text{ J cm}^{-3}$ has been reported for AF45 (Schott AG) [3] and OA-10G (Nippon Electric Glass Co. Ltd.) [1] ultra-thin glass-based capacitors, which is more than three times higher than that of the current state-of-the-art polymer-based capacitors. At a relatively high temperature of 300°C , at which traditional polymers such as polypropylene (PP) and polyethylene terephthalate (PET) are not usable, ultra-thin glass is stable and maintains a relatively low dielectric loss of $0.25\text{--}0.35\%$ [1], which is significantly lower than that of polyimide ($\tan \delta \sim 6\%$ at 300°C) - a typical high temperature polymer. Although the density of glass is about 2.5 times greater than PP [5], the benefits of the dielectric properties obtained from ultra-thin glass, especially at elevated temperature, may outweigh the density penalty. These attributes make ultra-thin glass a promising dielectric, especially for applications envisaged in the transport sector such as the more electric aircraft and hybrid/electric vehicles, wherein the capacitors might have to operate at relatively high ambient temperatures in order to meet advanced design requirements that offer a more energy efficient performance [6], [7], [8], [9].

Despite these attractive properties, research on ultra-thin glass based film capacitors is in its nascent stage. One of the main limitations of the current processing technology that is hindering the exploitation of glass-based capacitors is the inability to produce large area rolls of ultra-thin glass. The thinnest commercially available glass roll (up to 100 m long), which is $\sim 5 \mu\text{m}$ thick, is only about 5 mm wide [10] and hence limits the absolute capacitances attainable in a wound capacitor. The narrow strips also pose significant challenges during capacitor processing, particularly during masking, metallising, handling and winding. So relatively wide ($\sim 25 \text{ mm}$, which is usually the lower end of the width of polymer based capacitor films) and thicker ($\sim 10 \mu\text{m}$) glass-film rolls might be relatively easy to process, albeit at the cost of a loss in capacitance due to the increased thickness.

A simple approach to overcome these challenges and avoid the trade-off between film area and thickness is may be to enhance capacitance by increasing the surface area of the dielectric or capacitor electrode, and which does not involve increasing the width of the glass film. Such a modification, if well-controlled to obtain desirable high-surface area features, may offer a useful increase in capacitance.

Although a number of surface patterning and roughening techniques [11], [12], [13] are used to obtain high-surface area features, an ideal technique would be the one that will allow large-scale processing of surface features that are relatively easy to metallise via vacuum-based thermal evaporation [14], [15], [16], which is a widely used line-of-sight deposition technique for fabricating capacitors. A patterning technique that is compatible with thermal evaporation and large-scale roll-to-roll processing [16] would be preferred over techniques that involve multi-step, and relatively complex processes such as lithography, which might be difficult to economically scale-up.

In this paper we investigate how to enhance the dielectric properties of glass-based capacitors via a surface modification technique that involves a relatively simple process of ‘self-masking’ by thermal evaporation of non-wetting, self-organising nano-islands followed by preferential etching of ultra-thin glass [17], [13].

During vacuum deposition, noble metals such as Au and Ag do not ‘wet’ many substrate surfaces and tend to ‘roll-up’ to form nano-islands [18], [19] at deposition thicknesses of $< 10 \text{ nm}$. The self-organisation of this deposited metal into nano-islands can be used as a mask to preferentially etch the glass around the metal-islands, which is similar to the masking provided by polystyrene balls [13], and might result in the formation of ‘pillar’ or ‘peak’ like structures on

*This work was supported by an Innovate UK project – Power Electronic Inverters & Capacitors - Future Systems (PEICAP). Reference: 101664

Amoghavarsha Mahadevegowda, Colin Johnston, and Patrick Grant are with Department of Materials, University of Oxford, 16 Parks Road, Oxford OX1 3PH, United Kingdom.

[#]Email-id: amogh.gowda@materials.ox.ac.uk

subsequent etching. The selection of Ag for masking has two advantages: (i) deposition of Ag onto glass can be relatively easily incorporated into roll-to-roll processing, and (ii) any Ag that is left behind after etching can later become an integral part of the electrode during Al-metallisation unlike other impurities that have to be removed, for example where organics are used for masking.

Since the formation of the peak-like structures is facilitated by directional or anisotropic etching, a dry etching technique was preferred over wet etching. So we employed reactive-ion etching (RIE) to etch as-received and self-masked glass. The effect of self-masking by Ag and preferential etching were imaged and studied by atomic force microscopy (AFM) and scanning electron microscopy (SEM), and then correlated to the enhancement in dielectric properties.

II. EXPERIMENTAL

A. Fabrication

Ultra-thin glass (Schott AF 32) samples, 30 μm thick, were coated with a 10 nm thick layer of Ag (99.99% pure, Advent) on both sides at a rate of 0.1 nm/s in a Eurocoater thermal evaporator at a base pressure of 5×10^{-4} Pa. The thickness and deposition rate of the Ag layer was measured in real-time using a calibrated quartz crystal monitor. Reactive ion etching (RIE) of both sides of Ag-deposited glass was carried out in an Oxford Instruments Plasmalab80Plus under the conditions given in Table I.

TABLE I
REACTIVE ION ETCHING (RIE) CONDITIONS USED FOR ETCHING THE
ULTRA-THIN GLASS SAMPLES.

Ar (sccm)	25
CF ₄ (sccm)	25
Pressure (mTorr)	30
Etch duration (minute)	2, 5, 10
Microwave power (W)	100

B. Characterisation

AFM was performed on as-received and etched samples in Agilent Technologies and Park Systems microscopes, and scanning electron microscopy and energy-dispersive X-ray spectroscopy (EDS) were carried out in Hitachi-TM3000.

A layer of Al (40 nm thick) was deposited on both sides of the as-received and etched glass samples to make simple parallel-plate capacitors. Dielectric studies of these Al-metallised glass samples were carried out at 20 $^{\circ}\text{C}$ using a Solartron SI 1260 impedance analyser in the frequency range 100 Hz to 10 kHz.

III. RESULTS AND DISCUSSION

Figure 1 shows the variation of capacitance C of as-received and etched ultra-thin glass samples with etching time and frequency at 20 $^{\circ}\text{C}$. At 1 kHz, the capacitance of glass etched for 2 min (●) was approximately 8% higher than the capacitance of as-received glass (■). An increase in the etching time to 5 min led to a further increase by ~14%

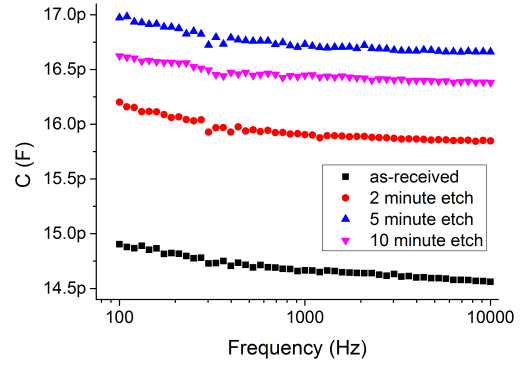


Fig. 1. Variation of capacitance C of as-received and etched ultra-thin glass samples with etching time and frequency at 20 $^{\circ}\text{C}$.

over the as-received glass. However, increasing the etching time to 10 min produced a similar increase of ~12%.

The dissipation factor $\tan \delta$ was measured and was in the range 0.002 to 0.006 at 1 kHz and 20 $^{\circ}\text{C}$ for all conditions, which was consistent with previous reports of $\tan \delta \sim 0.005$ [1], [20]. In order to understand the increase in capacitance of the etched glass-based capacitors, the surfaces were investigated by SEM-EDS and AFM.

Figure 2 shows SEM-EDS data from the glass samples at various stages of etching, with the corresponding weight percentage (wt.%) of surface Ag. The EDS data for as-received glass in Figure 2(a) showed no Ag peaks. After deposition with 10 nm of Ag, there were two characteristic Ag peaks [21]: $L\alpha_1$ at 2.98 keV and $L\beta_1$ at 3.15 keV, as seen in Figure 2(b). The surface Ag concentration was estimated as ~2.3 wt.% Ag, which decreased to ~1.7 wt.% Ag after 2 min of etching and then to ~1.0 wt.% Ag after 5 min of etching, as seen in Figures 2(c) and (d) respectively. A further increase in the etching time from 5 to 10 min did not result in a significant decrease in the Ag concentration, which remained at ~0.9 wt.% as seen in Figure 2(e). These results suggested that the RIE process, alongside any etching of the glass itself, was also removing some of the deposited Ag from the surface of the glass.

AFM was used to study the changes in topography resulting from Ag-deposition, Al-metallisation, removal of Ag from the surface by etching and etching effects on the glass itself. Figure 3 shows AFM images of the glass (a) as-received, (b) after Al metallisation, (c) after deposition of a nominally 10 nm of Ag on (a), and (d) after 10 min of RIE on (c) followed by Al-metallisation.

The measured root mean square roughness R_{rms} of as-received glass in Figure 3(a) was ~0.5 nm, which was consistent with $R_{rms} < 1$ nm quoted by the supplier for the fire-polished AF-32 glass [22]. The relatively light-shaded feature, ~100 nm size, circled in Figure 3(a) was most likely an impurity (for example a dust speck) sitting on the glass surface. After Al-metallisation in Figure 3(b), $R_{rms} \sim 0.5$ nm, suggesting that the evaporated Al deposited evenly across the relatively smooth glass substrate. However, after

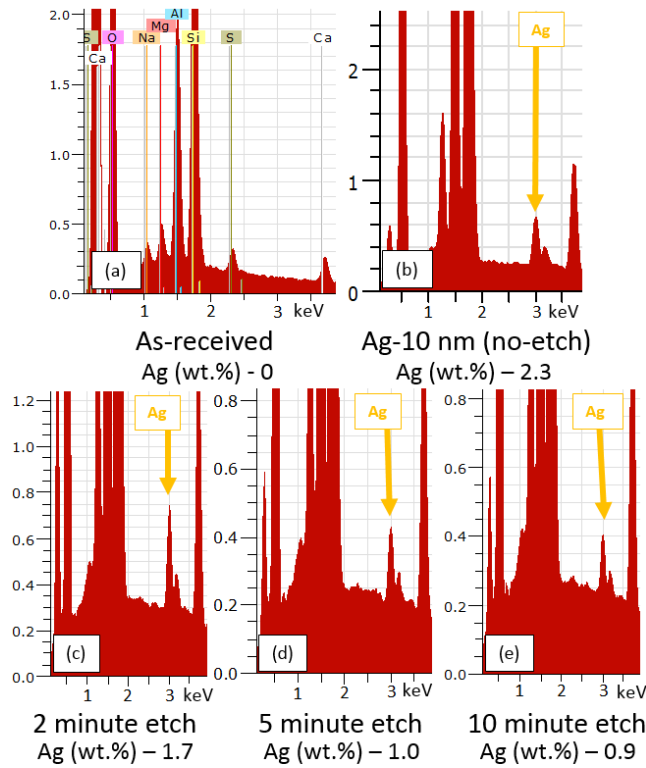


Fig. 2. SEM-EDS spectra from the glass surface at various stages of etching, with the corresponding estimate of weight percentage (wt.%) of Ag. These Ag measurements are semi-quantitative and give only a rough, relative estimate of the extent of Ag coverage on the surface.

deposition of nominally 10 nm of Ag, $R_{rms} \sim 1.8$ nm, indicating an approximate three time increase in roughness. This was interpreted and suggesting that while the Al ‘wets’ the surface, in contrast Ag has a higher contact angle with glass and tends to “ball” or “roll” up into discrete nano-islands on deposition, similar to the growth of deposited Ag on a polymer substrate such as nylon-6 [18], [19].

After etching in Figure 3(d), $R_{rms} \sim 4.5$ nm, indicating a 9 times increase in roughness over the as-received glass. The light-shaded feature circled in Figure 3(d) was relatively large at $\sim 0.8 \mu\text{m}$. So a relatively large area scan of $10 \mu\text{m} \times 10 \mu\text{m}$ was used for a further investigation.

Figure 4(a) is an AFM $10 \mu\text{m} \times 10 \mu\text{m}$ image of the same etched region in Figure 3(d) indicating many relatively large ($0.6\text{--}1 \mu\text{m}$), light-shaded features similar to the ones circled in Figure 4(a), distributed across the surface of the etched glass. Figure 4(b) is a three-dimensional (3D) AFM $10 \mu\text{m} \times 10 \mu\text{m}$ image of the “peaks” (circled) and Figure 4(c) shows a relatively high-resolution AFM image of a peak (circled). The peaks themselves do not have smooth sides, as seen in Figure 4(c). The height and width of the peaks measured from a line profile shown in Figure 4(d), along the two peaks in Figure 4(a), were ~ 25 nm and $\sim 1 \mu\text{m}$ respectively.

The presence of the peaks can be explained as follows with reference to the schematic shown in Figure 5: the deposited Ag formed spheres or islands on the surface of glass instead of forming a continuous layer as Ag does not ‘wet’ the

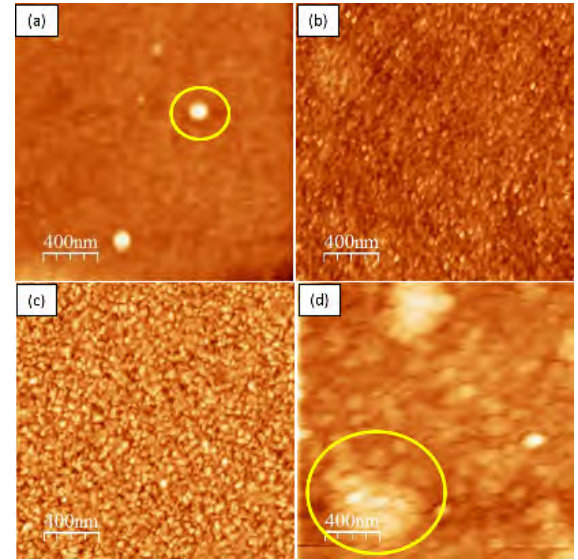


Fig. 3. AFM images of (a) as-received glass, (b) Al-metallised glass, (c) the same glass in (a) but with nominally 10 nm of deposited Ag, and (d) the same glass in (c) but now etched for 10 min and then Al-metallised.

surface [18], [19], which was supported by their increased R_{rms} . The Ag-islands partially masked the surface of glass during etching as shown in Figure 5(a), and the regions around the Ag-islands were more heavily etched than regions under the Ag-islands. Although Ag was also etched away with time, the preferential etching around the Ag-islands resulted in the formation of peaks shown in Figure 5(b), which led to the nearly ten fold increase in R_{rms} and the surface area.

Since evaporated Al is shown to form relatively smooth films [23] at low deposition rates of ~ 0.1 nm/s, which follow the contour of the substrate, it is reasonable to assume that on subsequent metallisation, Al covered the etched surface and provided an overall increase in the area of the electrodes that formed the parallel plate capacitor. This increase in the area increased dielectric properties, as shown in Figure 1, with a highest increase in capacitance of $\sim 14\%$.

The enhanced capacitance of our glass-based dielectrics is greater than previous reports [1], [3], [4] and makes use of a processing technique involving vacuum deposition that might also be applied to fabricate capacitors with different electrodes such as MnO_2 to further improve the performance and reliability [2].

IV. CONCLUSIONS

We successfully employed a vacuum deposition based self-masking technique, which has been suggested to be compatible with roll-to-roll processing, followed by preferential etching to enhance the dielectric response of glass-based capacitors. AFM and SEM-EDS investigation of the self-masking effect provided by Ag nano-islands showed that preferential etching resulted in the formation of increased surface area features, such as nano-sized peaks, and provided an increase in capacitance of glass-based dielectrics by 14%.

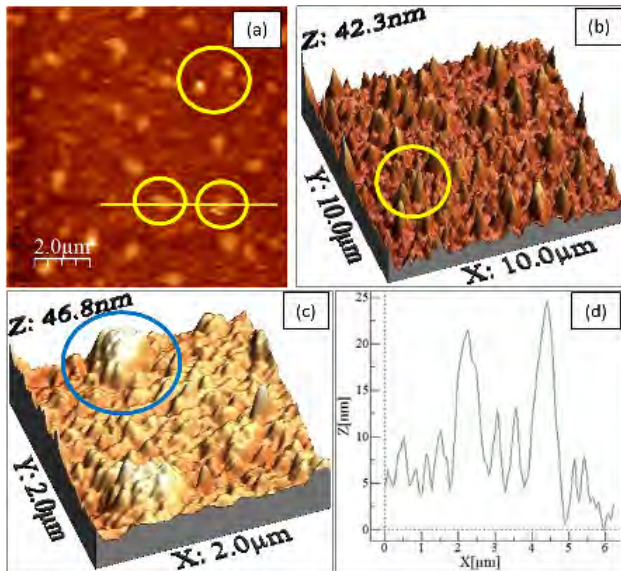


Fig. 4. (a) An AFM $10\ \mu\text{m} \times 10\ \mu\text{m}$ image of etched glass; (b) a three-dimensional AFM $10\ \mu\text{m} \times 10\ \mu\text{m}$ image of the etched glass with peaks (circled) distributed across the surface; (c) a high-resolution AFM image of the peak (circled); and (d) a line profile along two peaks circled in Figure 4(a).

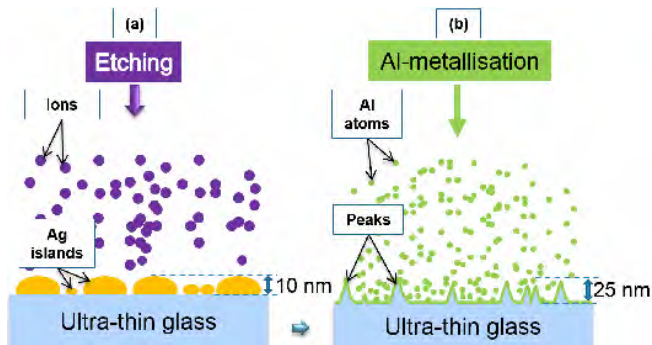


Fig. 5. A schematic representation of the roughening process showing (a) etching of the Ag-masked glass and (b) Al-metallisation of the preferentially etched glass surface with peaks.

ACKNOWLEDGMENTS

This work was funded by an Innovate UK project – Power Electronic Inverters & Capacitors - Future Systems (PEICAP) consisting of the following partners - Safran Electrical & Power UK Ltd, University of Oxford, Industrial Capacitors Wrexham Ltd, and Raytheon UK. IUK Reference: 101664

REFERENCES

- [1] M. P. Manoharan, C. Zou, E. Furman, N. Zhang, D. I. Kushner, S. Zhang, T. Murata, and M. T. Lanagan, "Flexible Glass for High Temperature Energy Storage Capacitors," *Energy Technology*, vol. 1, p. 313, 2013.
- [2] B. Akkopru-Akgun, S. Troler-McKinstry, and M. T. Lanagan, "MnO₂ Thin Film Electrodes for Enhanced Reliability of Thin Glass Capacitors," *Journal of the American Ceramic Society*, vol. 98, no. 10, p. 3270, 2015.
- [3] N. J. Smith, B. Rangarajan, M. T. Lanagan, and C. G. Pantano, "Alkali-free glass as a high energy density dielectric material," *Materials Letters*, vol. 63, p. 1245, 2009.
- [4] T. Murata, P. Dash, E. Furman, C. Pantano, and M. Lanagan, "Electrode-Limited Dielectric Breakdown of Alkali Free Glass," *Journal of the American Ceramic Society*, vol. 95, no. 6, p. 1915, 2012.
- [5] T. Murata, T. Yanase, S. Miwa, and H. Yamazaki, "Ultra thin glass roll for flexible AMOLED display," *Proceedings of 18th International Display Workshop 2011 - FMC8 - Manufacturing Technologies*, vol. 18, p. 1735, 2011, Nagoya, Japan, 7-9 December 2011.
- [6] M. Howse, "All-electric aircraft," *Power Engineer*, vol. 17, no. 4, p. 35, 2003.
- [7] R. Johnson, J. Evans, P. Jacobsen, J. Thompson, and M. Christopher, "The changing automotive environment: High-temperature electronics," *IEEE Transactions on Electronics Packaging Manufacturing*, vol. 27, no. 3, p. 164, 2004.
- [8] H. Wang and F. Blaabjerg, "Reliability of capacitors for DC-link applications in power electronic converters - An overview," *IEEE Transactions on Industry Applications*, vol. 50, no. 5, p. 3569, 2014.
- [9] H. Wen, W. Xiao, X. Wen, and P. Armstrong, "Analysis and evaluation of DC-link capacitors for high-power-density electric vehicle drive systems," *IEEE Transactions on Vehicular Technology*, vol. 61, no. 7, p. 2950, 2012.
- [10] Nippon Electric Glass: Super thin glass-ribbon. (Last accessed: July 19, 2016) Webpage - <http://www.neg.co.jp/epd/opt/eng/seihin/glass-ribbon.html>.
- [11] D. Jang and J. R. Greer, "Transition from a strong-yet-brittle to a stronger-and-ductile state by size reduction of metallic glasses," *Nature Materials*, vol. 9, no. 3, p. 215, 2010.
- [12] Z. Yoshimitsu, A. Nakajima, T. Watanabe, and K. Hashimoto, "Effects of surface structure on the hydrophobicity and sliding behavior of water droplets," *Langmuir*, vol. 18, no. 15, p. 5818, 2002.
- [13] W. Li, L. Xu, W.-M. Zhao, P. Sun, X.-F. Huang, and K.-J. Chen, "Fabrication of large-scale periodic silicon nanopillar arrays for 2D nanomold using modified nanosphere lithography," *Applied Surface Science*, vol. 253, no. 22, p. 9035, 2007.
- [14] A. Mahadevegowda, N. Young, and P. Grant, "Engineering the nanostructure of a polymer-nanocomposite film containing Ti-based core-shell particles to enhance dielectric response," *Nanoscale*, vol. 7, no. 38, p. 15727, 2015.
- [15] A. Mahadevegowda, N. P. Young, and P. S. Grant, "Core-shell nanoparticles and enhanced polarization in polymer based nanocomposite dielectrics," *Nanotechnology*, vol. 25, no. 47, p. 475706, 2014.
- [16] J. Affinito, P. Martin, M. Gross, C. Coronado, and E. Greenwell, "Vacuum deposited polymer metal multilayer films for optical application," *Thin Solid Films*, vol. 270, no. 1-2, p. 43, 1995.
- [17] E. Hein, D. Fox, and H. Fouckhardt, "Glass surface modification by lithography-free reactive ion etching in an Ar/CF₄-plasma for controlled diffuse optical scattering," *Surface & Coatings Technology*, vol. 205, no. 2, p. 419, 2011, 12th International Conference on Plasma Surface Engineering, Garmisch-Partenkirchen, Germany, September 13-17, 2010.
- [18] A. Mahadevegowda, N. P. Young, and P. S. Grant, "Electron microscopy of multi-layered polymer-nanocomposite based dielectrics," *Journal of Physics: Conference Series*, vol. 522, p. 012041, 2014.
- [19] J. A. Venables, G. D. T. Spiller, and M. Hanbucken, "Nucleation and growth of thin-films," *Reports on Progress in Physics*, vol. 47, no. 4, p. 399, 1984.
- [20] M. P. Manoharan, M. T. Lanagan, S. Zhang, D. Kushner, C. Zhou, and T. Murata, "High temperature - High energy density polymer-coated glass capacitors," in *IEEE Transportation Electrification Conference and Expo, ITEC 2013, Metro Detroit, MI, USA*, 16-19 June 2013.
- [21] W. L. Ong, Y.-F. Lim, J. L. Ting Ong, and G. W. Ho, "Room temperature sequential ionic deposition (SID) of Ag₂S nanoparticles on TiO₂ hierarchical spheres for enhanced catalytic efficiency," *Journal of Materials Chemistry A*, vol. 3, p. 6509, 2015.
- [22] Technical Details: Schott - AF 32 eco Thin Glass. (Last accessed: July 19, 2016) Webpage - <http://www.us.schott.com>.
- [23] N. G. Semaltianos, "Thermally evaporated aluminium thin films," *Applied Surface Science*, vol. 183, p. 223, 2001.